INTELLIGENT CONTROL BASED FRT CAPABILITY OF NINE SWITCH GRID SIDE CONVERTER FED DFIG SYSTEM

M. Nirmala, Dr.K.Baskaran
Research Scholar, Anna university,Tamilnadu, India,
Government college of technology ,Coimbatore, Tamilnadu,India
m.nirmala.gct@gmail.com,9894524985

Abstract— The large-scale integration of wind power in today's power system, the main provocation for wind turbine to give Fault Ride-Through (FRT) capability. To meet the present grid codes, wind turbine should sustain the grid voltage by the reactive power control. The main shortcoming of conventional FRT capability of DFIG with rotor crowbar system would absorb reactive power from grid during grid fault. The proposed work is an Adaptive Neural Network(ANN) intelligent controller based FRT capability of Dual output Grid Side Nine Switch Converter(GSNSC) fed Doubly Fed Induction Generator during LLLG grid faults. The conventional Grid Side Six Switch Converter (GSSSC) are replaced by Dual Output converter(DOC). The DOC can provide six autonomous output terminals with the help of additional three switches. The upper output terminals are connected to the grid while, the bottom output terminals are connected to neutral side of stator windings to provide FRT capability to the DFIG. The impact performance of the ANN based controller is then compared with that of fuzzy based controller and conventional PI controller. Simulation results of 1.5-MW WECS are conceded out in Matlab/Simulink.

Keywords— ***Wind energy conversion system(WECS), Doubly fed induction generator(DFIG), Grid Side Nine Switch Converter(GSNSC), Grid Side Six Switch Converter (GSSSC), Adaptive Neural Network(ANN),Fuzzy Logic Controller(FLC).***

I. INTRODUCTION

Now a days, the worldwide research area is sustainable, efficient and Green power renewable energy [1–2]. Wind power is the most rapidly growing one in the world among various renewable energy sources. The wind is random and intermittent, and the lack of efficient control. The doubly fed induction generator (DFIG) based wind turbines more widely used in large wind farms. There are several advantage such as the increasing number of WECS connected to the grid are converter with reduced power rating and capability to provide power at constant voltage and frequency even as the rotor speed varies and reduced costs and losses, improved efficiency, easy power factor correction compared with fixed speed generator[3].

In the DFIG, stator windings are directly connected to the power grid and via the AC-DC-AC converter, the rotor is connected to the power grid in which converter rating about 20–30% of the DFIG rated capacity that supplies the exciting current of the DFIG only. The AC-DC-AC converter consists Rotor Side Converter(RSC), Grid Side Converter(GSC) and DC Link capacitor. But the stability of grid-connected DFIG is effected by the controller of the converter operation[4,5].

FRT requires DFIG to stay online for a definite time during voltage dips for preventing excess generated power loss and a subsequent drop of system frequency. The prescribed length of time before the unit is allowed to disconnect if voltage is not restored depends on the magnitude of the initial value of voltage sag. Depends on Grid code, Voltage sags are calculated at the point of common coupling of a wind power plant or at generator terminals. The various requirements are concerned rely type of fault and protection systems used in the grid. Time-voltage diagrams ('FRT envelopes') are used to describe the exact conditions allowing or prohibiting disconnection. FRT envelope examples from various grid codes[6] are illustrated in Fig.1.

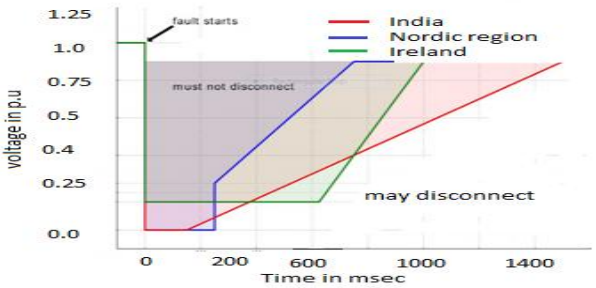

Fig. 1. FRT Envelopes from various grid codes

There are several approaches to apply for the FRT capability of the DFIG wind turbine. A bypass resistor has been used to enhance the FRT capability[7] While many papers can be found in the literature look into different ways for reactive power compensation in WECS during fault events by mainly connecting a flexible AC

transmission system (FACTS) device such as static synchronous compensator (STATCOM) to the PCC [8-10], a few publications considered the compensation of active power as well [11,12].

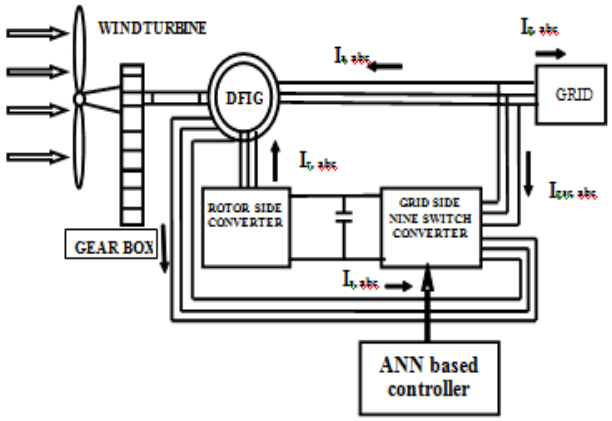

Fig. 2. ANN based fault tolerant configuration of DFIG

However, during faults the partially rated converters shall be capable of riding-through the transient currents and voltages. During a fault incident, the voltage drops to zero and the active power generation is reduced leading to rapid increase in the rotor current in an attempt to compensate the active power by the rotor side converter (RSC). Hence, the converter increases the rotor voltage which leads to an overvoltage in the dc link [13], [14]. When the crowbar is engaged, the DFIG behaves like an induction machine since the rotor winding is short-circuited by shunt resistors and the RSC is disabled [15]. The drawback of crowbar applications is obviously that the DFIG consumes reactive power and might worsen the grid voltage during faults [16]. Other approaches focus on limiting the rotor currents by employing the dynamic series braking resistor in coordination with the crowbar [16], [17].

To achieve FRT operation in wind system with recent grid codes using a ANN based fault-tolerant configuration of DFIG using a Grid Side Nine-Switch Converter (GSNSC) is proposed as is shown in Fig.2. An appropriate control algorithm for the control of a nine-switch converter is developed to maintain the stator flux. The reactive current support in line with recent grid code requirements during the grid fault conditions[18], an ANN based reactive power controller is developed to share reactive current between GSNSC and RSC during any kind of grid fault .

II. MODELING OF SIX TERMINAL STATOR OF DFIG

A. *Grid Side Nine Switch Converter*

The circuit of the Rotor Side Converter and Grid side Nine switch converter are shown in Fig.3. The stator windings are directly connected to grid and the rotor windings are connected to the RSC (switches Q1–Q6). The RSC in the proposed configuration shares the dc link capacitor (C) with additional switches of the Grid Side Nine Switch converter (switches T1–T9) instead of traditional Grid side converter which has only six switches. The upper output of the GSNSC is connected to grid via interfacing inductor while, the lower output is connected to the neutral side of the stator windings of the DFIG. The lower three switches Of GSNSC (T3, T6, and T9)

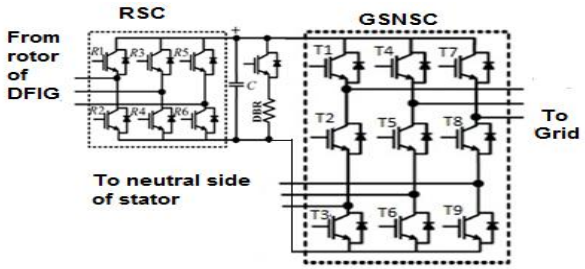

Fig. 3. New Structure of AC-DC-AC Converter of DFIG

are short circuited to form the star-point of the stator windings during the normal operation while, the upper 6 switches (T1,T2, T4,T5, T7 and T8) are controlled as a conventional six switch GSC to regulate the dc-link voltage. Dc link voltage is controlled by using Dynamic Braking Resistor.

During the grid faults, the voltage value falls to below 0.9 p.u in grid .The lower three switches (T3, T6, and T9) also start switching to generate the compensating voltages on the neutral side of the stator winding to maintain pre-fault voltage across it. This operation of generating the compensating voltages on the neutral side of the stator winding is termed here as Neutral Side Converter (NSC) operation. During voltage sag, the NSC will take up part of the active power generated by DFIG and forces it to the dc link, hence, dc-link voltage tends to increase if any preventive measures are not taken. DFIG with six stator terminal is modeled by using rotor reference frame [19]. The voltage and flux equations of stator and rotor of DFIG with the six terminal stator in rotor reference frame can be written as follows:

Using the d-axis and q-axis component of stator voltage of grid side(u_{ds} and u_{qs}) and neutral side of the stator voltages (u_{dn} and u_{qn}), the stator voltage equation is written as

$$u_{ds} - u_{dn} = R_s i_{ds} + \frac{\mathrm{d}\psi_{ds}}{\mathrm{dt}} - \omega\psi_{qs} \qquad (1)$$

$$u_{qs} - u_{qn} = R_s i_{qs} + \frac{\mathrm{d}\psi_{qs}}{\mathrm{dt}} - \omega\psi_{ds} \qquad (2)$$

Where the variables i_{ds} and i_{qs} represent the stator currents, while R_s , ψ_{ds} $\psi_{qs}$and ω are represents stator resistance, the d and q axis component of stator flux and supply frequency .The d-axis and q-axis component of rotor voltage of DFIG can be written as

$$u_{dr} = R_r i_{dr} + \frac{d\psi_{dr}}{dt} - (\omega\psi_{qr} - \omega_r\psi_{qr}) \quad (3)$$

$$u_{qr} = R_r i_{qr} + \frac{d\psi_{rq}}{dt} + (\omega\psi_{dr} - \omega_r\psi_{dr}) \quad (4)$$

Where the variables i_{dr} and i_{qr} represent the rotor currents, while R_r , ψ_{dr},$\psi_{qr}$and ω_r are represents rotor resistance, the d and q axis component of rotor flux and rotor angular frequency. The d –axis and q-axis component of stator flux can be calculated as:

$$\psi_{sd} = (L_m I_{sd} + L_m I_{rd}) + L_s i_{ds} \quad (5)$$

$$\psi_{sq} = L_s i_{qs} + (L_m I_{sq} + L_m I_{rq}) \quad (6)$$

$$\psi_{rd} = (L_m I_{ds} + L_m I_{rd}) + L_r i_{dr} \quad (7)$$

$$\psi_{rq} = L_r i_{qr} + (L_m I_{qs} + L_m I_{qr}) \quad (8)$$

L_s , $L_r$and L_m represent the self-inductance of stator, self-inductance of rotor and mutual inductances referred to stator winding, respectively. The basic expressions for the electromagnetic torque developed in DFIG and stator reactive power in terms of rotor variables by aligning the d-axis of the reference frame to the air-gap flux, can be written as

$$T_e = \frac{(\psi_{ds} L_m) i_{qr}}{L_s} \quad (9)$$

$$Q_s = \frac{(u_{ds}\varphi_{ds})}{L_s} - \frac{(u_{ds} L_m) i_{dr}}{L_s} \quad (10)$$

The equation (9) and (10) state that, the electromagnetic torque developed is directly proportional to the q-axis rotor current while the stator reactive power is directly proportional to the d-axis rotor current. The decoupled control of i_{dr} and i_{qr} , the active power (or electromagnetic torque) and the stator reactive power can be controlled independently by RSC.

III. Control Strategies of DFIG

A. *Normal Mode operation of AC-DC converter at RSC Control:*

The electromagnetic torque and hence active power produced by DFIG is proportional to i_{qr} can be regulated by controlling u_{qr} . The reactive power produced by DFIG is proportional to i_{dr} regulated by controlling v_{dr}. The detailed control diagram of RSC is shown in Fig. 4. The q-axis command quantity of rotor current $i_{qr}{}^*$is calculated from the $T_e{}^*$ generated using a PI controller over the rotor speed. Using maximum power point Tracking (MPPT) algorithm, the speed command signal $\omega_r{}^*$can be produced. The d-axis command quantity of rotor current $i_{dr}{}^*$is generated using a PI controller over reactive power supplied by the DFIG. The rotor command current $i_{dr}{}^*$ is endorsed to confine any value within the limits in order to take out the maximum power from WT while it is limited to ensure RSC current is within the safe limit in the normal mode of operation. The command rotor currents $i_{dr}{}^*$ and $i_{qr}{}^*$ are tracked using decoupled PI current control by regulating v_{dr} and v_{qr} as per (5-8). The command RSC voltage signal is compared with a high frequency carrier wave using a sinusoidal pulse width modulation (SPWM) technique which produce gating signal for RSC.

B. *Fault Mode operation at RSC Control:*

The main aim of RSC control is toggled to provide full reactive current within safe value which is obtained by dipping stator active current lower the safe limit. This leads very high rotor speed which developed mechanical stress in wind turbine. The wind turbine mechanical stress is reduced by as follows:

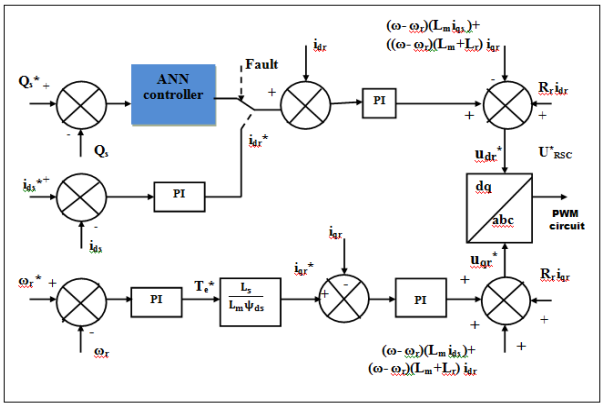

Fig. 4. Rotor Side Converter control circuit

Stator supplies two-third of the reactive current supplied and RSC supplies one-third of reactive current. The reactive current distribution is intended using the PI controller over command stator reactive current under fault mode of operation. If the grid voltage V_g is 0.5 to 0.9 p.u, then the I_{ds}* is equal to (1.35-1.5V_g) if else the I_{ds}* is equal to – 0.6.

C. *Normal mode operation of GSNSC Converter:*

The object of the GSC is to regulate the dc-link voltage to its reference value irrespective of direction of rotor power flow and its circuit is shown in Fig.5.Using synchronous reference frame, the voltage balance equation across interfacing inductor (L) with internal resistance(R) can be written as

$$u_{d,O1GSC}{}^* = Ri_{dg} + L\frac{di_{dg}}{dt} - \omega L i_{qg} + u_{gd} \quad (11)$$

$$u_{q,O1GSC}{}^* = Ri_{qg} + L\frac{di_{qg}}{dt} - \omega L i_{dg} + u_{qg} \quad (12)$$

The GSC supplies or absorbs the active and reactive power can be written as

$$P = \frac{3}{2} i_{dg}\, u_{dg} \quad (13)$$

$$Q = \frac{3}{2} i_{qg}\, u_{dg} \qquad (14)$$

By controlling the signal $u_{d,O1GSC}{}^{*}$, active power can be regulated whereas by controlling the signal $u_{q,O1GSC}{}^{*}$,the reactive power can be regulated. The Grid side d-axis command current signal $i_{dg}{}^{*}$is generated using PI controller over average dc-link voltage and the Grid side q-axis command current $i_{qg}{}^{*}$is set equal to zero.

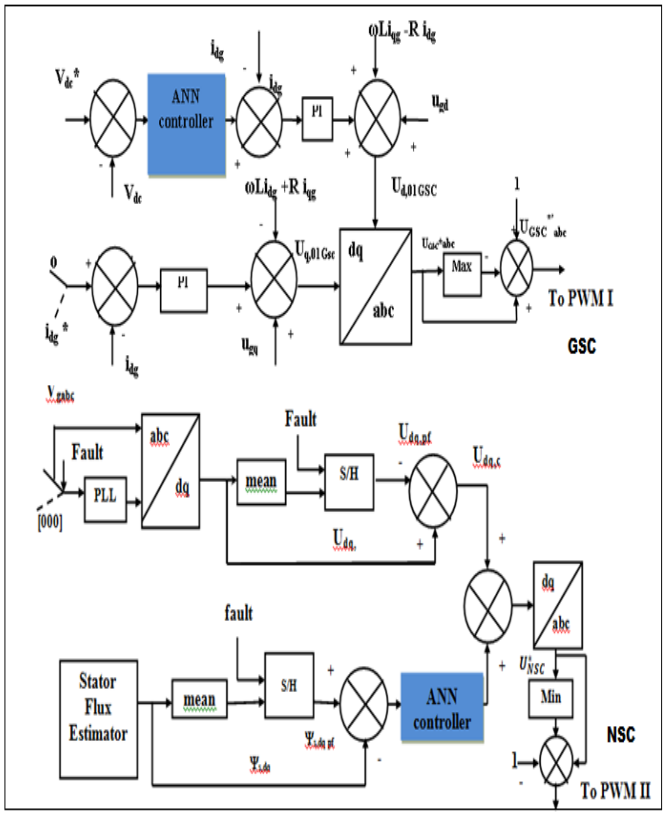

Fig. 5. Grid Side Converter Control circuit

By employing decoupled current control as per equation (13) and (14), the GSC generates the reference voltage $u_{O1GSC}{}^{*}$ in order to control GSC current to its reference value is computed. During normal operation (no fault) the voltage to be injected by GSC the second output at neutral side of the stator winding is zero. Hence, in the normal mode of operation, the Neutral side converter controller is inactive and the reference voltage to be generated by the GSNSC converter $u_{GSC}{}^{*}$ is kept equal to zero. For the phase-A output is obtained [19] by following switching technique shown in Table I. By proper design of the modulating signal, the problem of short circuit is avoided by using two modulating signals which are in phase with each other.

TABLE I SWITCHING CONTROL OF PHASE –A OF GSNSC

GSNSC outputs	T1	T2	T3	Phase-A connected to
Both outputs	high	High	low	+Vdc
Both outputs	low	High	high	0V
First o/p	high	Low	high	+Vdc
second o/p	high	Low	high	0V
First output	high	High	high	Short circuit the Vdc

Hence the first modulating signal constantly above that of the second modulating terminal by adding offsets to both the references. The control signals can be obtained by using reference signals as follows:

$$u_{GSC}{}^{*\prime}{}_{abc} = u_{GSC}{}^{*}{}_{abc} + [1 - \max(u_{GSC}{}^{*}{}_{abc})] \qquad (15)$$

$$u_{NSC}{}^{*\prime}{}_{abc} = u_{NSC}{}^{*}{}_{abc} + [1 + \min(u_{NSC}{}^{*}{}_{abc})] \qquad (16)$$

The three-phase PWM generators PWM-I and PWM-II are generates the two different sets of six PWM signals by using control signals$u_{GSC}{}^{*\prime}{}_{abc}$ and $u_{NSC}{}^{*\prime}{}_{abc}$. However, in a GSNSC converter, the middle three switches are shared by both controller from which gate pulses are generated by using logical EXOR operation of PWM signals corresponding to lower three switches by PWM-I and upper three switches by PWM-II. During normal mode, the switches T3,T6.and T9 switches are ON, and these create the stator windings on neutral side to form the star point.

D. *Fault mode operation of GSNSC Converter:*

To maintain a pre-fault voltage across the stator winding, the NSC output is controlled while the RSC and GSC control is switched to supply reactive current in line during the fault mode of operation. By measuring the absolute error$\{1 - u_{gabc}\}$ between reference grid voltage magnitude and actual grid voltage magnitude, the fault in the system can be detected almost instantaneously .The grid fault is detected at any time , the grid voltage exceeds the threshold (typically 0.1 p.u.). Once the grid fault is detected, the signals from PWM_1 and PWM_2 logic changed from 0 to 1.

E. *Nine-Switch Converter Control During Fault Mode:*

If the grid voltage V_g is $0.5 < V_g < 0.9$ p.u , then the q – axis stator reference current for the GSC is equal to -$(0.675\text{-}0.75V_g)$ if else the current is equal to -0.3. The objective of the neutral side converter control is to keep the pre-fault voltage across the stator winding for the proper functioning of the RSC control during fault condition. The injected compensating voltage is calculated by subtracting pre fault voltage from total dq- component of stator voltage. When fault is detected, the pre-fault stator flux components are obtained by holding the samples of two cycle mean value using sample and hold circuit as shown in Fig.6.

IV. PROPOSED ANN BASED CONTROLLER

The main action of PI controller consider only instantaneous value of error and not for derivative of the error. The PI controller increases the maximum overshoot of the system and also leads to unstable under stator flux variation. During the grid fault condition, the neutral side converter controls the variation of the stator flux by means of conventional PI controller. The input of the PI controller is error signal obtained by comparison of the stator flux value in both regular mode and fault mode of operation of DFIG. The controller reduces the steady state error and provides the output signal for the production of the gating signal to PWM II generator for the operation of NSC. During the fault, the transient change in stator flux, there is a change in increase and decrease error value, the PI controller cannot response immediately. The dc link voltage (Vdc) and stator reactive power also variable during fault mode of operation of DFIG. The PI controller response is not adequate during the variation of DFIG. To improve the performance of the system, in Fig.4., Fig.5. and Fig.6 PI controllers are replaced with ANN based controller. The most popular method of training is the back propagation (BP) algorithm used in feed forward Multilayer Neural Networks (MNN)[20].

In the proposed work, the input-output data are essential for neural network which is trained in off-line. The data set is sufficiently loaded to achieve stable operation by using Levenberg-Marquardt back propagation learning algorithm[21] as shown in Fig.7. The main advantage of algorithm is compared to other method, it occupies less memory space and also most admired supervised learning rule for feed forward networks especially suitable for multi-layer. Frequently input data is obtainable to the neural network. For each input, an error is calculated by the output of the neural network is compared with the target output. The neural network back propagates the error and adjust the weights such that the error reduces with every epochs and the neural network output gets almost target output. The main objective of this algorithm is to reduce the Mean Square Error(MSE) as shown in Fig.6.

V. SIMULATION AND RESULTS

The main problem of Grid Side six switch inverter based DFIG is increase in stator flux during grid fault condition, the post fault voltage results in high current in the WECS system. To overcome this shortcoming, a Grid Side Nine Switch Inverter has been used to maintain the pre-fault voltage across the stator winding during grid faults. The value of the proposed DFIG wind turbine configuration and its control to complete fault lenient operation is validated, an extensive simulation study is carried out in MATLAB. The detailed model of DFIG with six-terminal stator and the nine switch Grid side power electronics converters are developed using SIMULINK and Sim Power Systems tool-boxes**.** The real operating conditions is represented that the DFIG wind turbine is connected to a 120 kV grid through a (575 V-Yg/25) kV step-up transformer 25 kV–30 km, a transmission line and 25 kV /120 kV-Yg another step-up transformer. The wind turbine specifications and machine parameters used are tabulated in Table II.

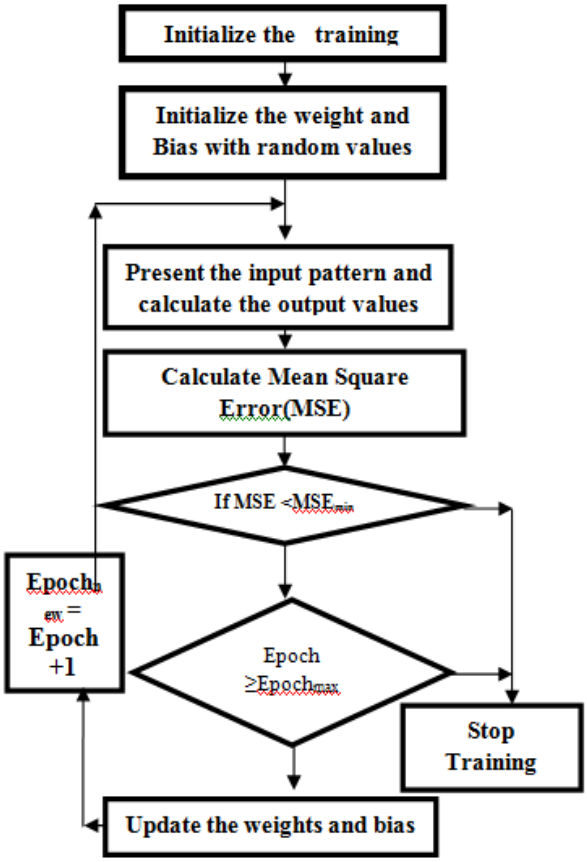

Fig. 6. Flow chart for Levenberg – Marquardt algorithm

TABLE II DFIG AND WIND TURBINE PARAMETERS

Nominal output power	1.5MW
Rated Wind Speed	15m/s
Operating Range	6-30m/s
nominal line-line voltage (Vrms)	575 V
nominal frequency (fnom)	60 Hz
stator resistance (rs)	0.0023pu
stator inductance (Ls)	0.18pu
rotor resistance (rr)	0.0016 pu
rotor inductance (Lr)	0.16 pu
mutual inductance (Lm)	2.9 pu
Number of poles	6
Inertia constant (H)	0.685
Friction factor (F)	0.01 pu

A. CONVENTIONAL PI CONTROL BASED NINE SWITCH INVERTER FED DFIG

The performance of the proposed fault- tolerant DFIG configuration is evaluated under LLLG faults at 25kV bus and the corresponding results are shown in Figs. 11–12. To prove the compatibility of the proposed configuration with recent grid codes for the effective fault ride through, faults are emulated for the duration of 100ms. All of the results are represented in per unit for a wind speed of 12 m/s. The system is under steady state before the simulation time of 0.3 s.

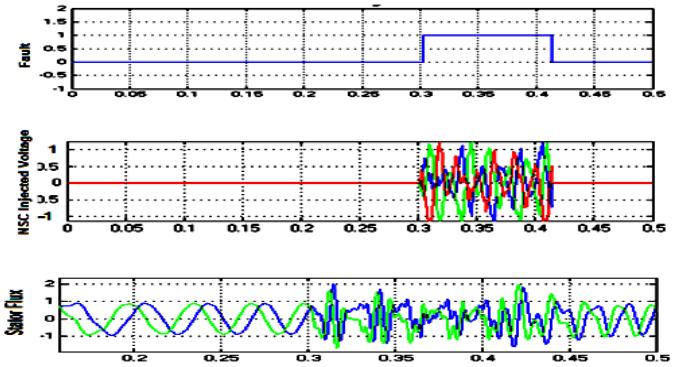

Fig. 7. Grid Fault, NSC injected voltage and stator Flux for PI controller based Nine switch inverter fed DFIG during LLLG fault

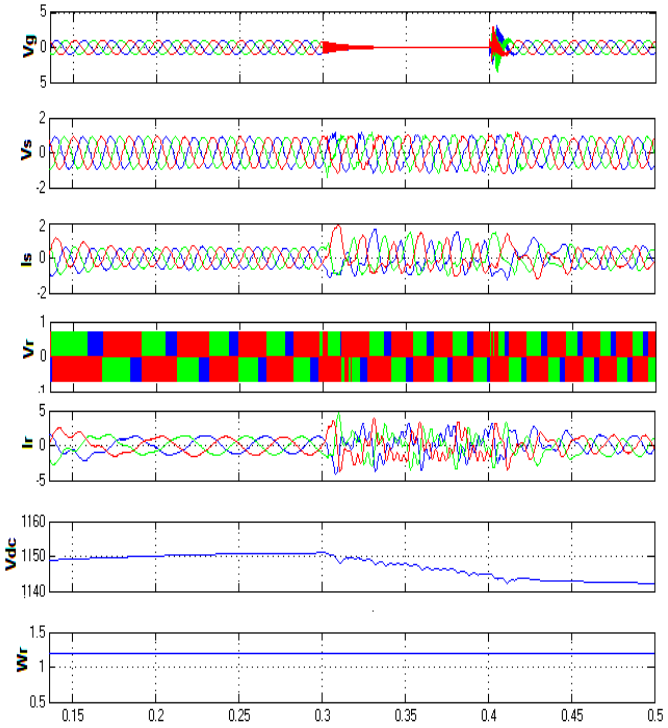

Fig. 8. Grid Voltage, stator voltage and current, Rotor voltage and current, dc link voltage, rotor speed for PI controller based Nine switch inverter fed DFIG during LLLG fault

Fig.7. represents that, the stator flux value in DFIG is increased beyond the 1 p.u due to presence of dc component during LLLG fault even the NSC injected increased beyond the 1 p.u due which is slightly distorted in conventional PI controller based Nine switch inverter fed DFIG . Fig.8 illustrates that the stator and rotor voltage and current are more distorted.

B. FUZZY PI CONTROL BASED NINE SWITCH INVERTER FED DFIG

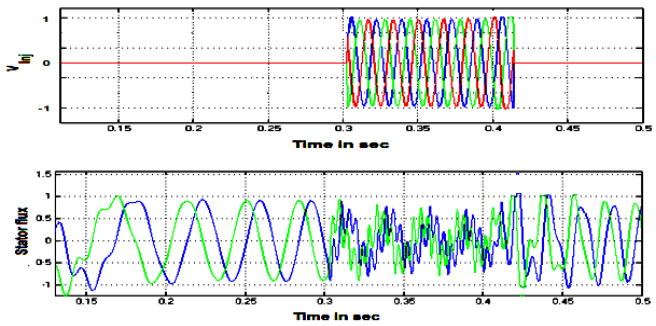

Fig. 9. NSC injected voltage and stator Flux for Fuzzy PI controller based Nine switch inverter fed DFIG during LLLG fault

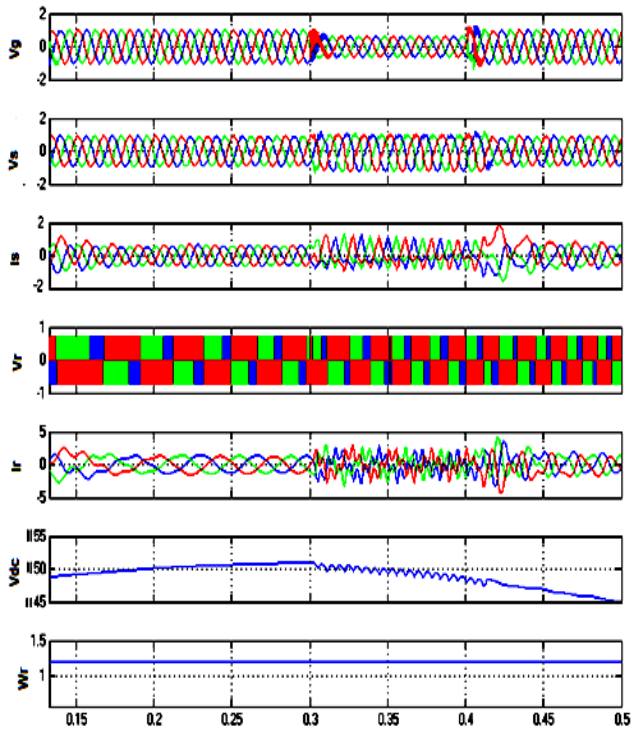

Fig. 10. Grid Voltage, stator voltage and current, Rotor voltage and current, dc link voltage, rotor speed for Fuzzy PI controller based Nine switch inverter fed DFIG during LLLG fault

Fig. 9 and Figure 10 shows the dynamic response of the DFIG based WECS under LLLG fault conditions when provided with the proposed fuzzy logic controllers as compared with the conventional PI controllers of optimal gains. It can be observed that the stator flux is limited within p.u and voltage injected at the neutral side of stator winding is transient free operation compared to conventional controller, but the d axis and q axis quantities of stator flux waveforms are irregular, not a pure sinusoidal waveform. Even though the stator and rotor currents are limited to a safe value below the transient current, there is distortion during transient period as shown in Fig.10.

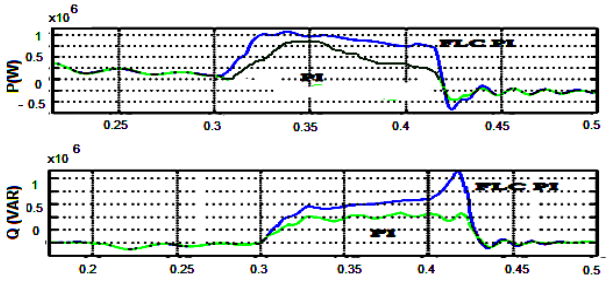

Fig. 11. Real power and reactive power injected to grid using Fuzzy PI controller based Nine switch inverter fed DFIG during LLLG fault

From Fig.11, it can be observed that during the voltage sag period and the instants after clearance of the fault, there are some small fluctuations in active and reactive power but the system recovers to its good stability state. The NSC injects 1 MW active power and 1MVAR reactive power. By inspection of the dynamic response, it can be realized that the dynamic response of the DFIG based wind system when provided with the fuzzy logic controllers has maximum percentage overshoot lower than that experienced by the PI controllers.

The fuzzy logic controllers improve the system damping after the first overshoot in comparison with that of the PI controllers. It also yields a much faster response that allows the system to reach the steady state after 0.42s, while in the PI technique it reaches the steady state after 0.45 s. Also the stator flux is limited within the value of p.u and NSC injects p.u voltage during fault period.

C. ANN CONTROL BASED NINE SWITCH INVERTER FED DFIG

Fig.12 and Fig.13 shows that the dynamic response of the DFIG based WECS under LLLG fault conditions when provided with the proposed ANN controllers as compared with the Fuzzy PI controllers of optimal gains.

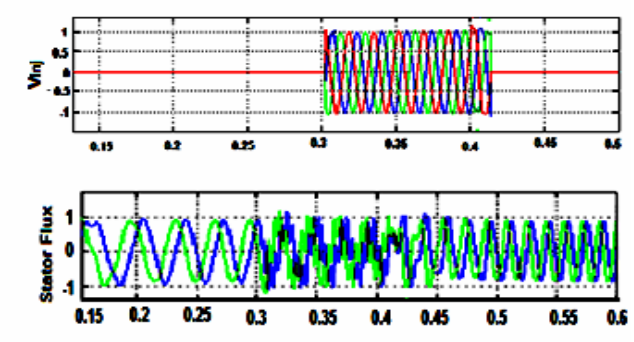

Fig. 12. Real power and reactive power injected to grid using ANN controller based Nine switch inverter fed DFIG during LLLG fault

It can be observed that the stator flux is limited within p.u, and voltage injected at the neutral side of stator winding is transient free operation compared to conventional controller

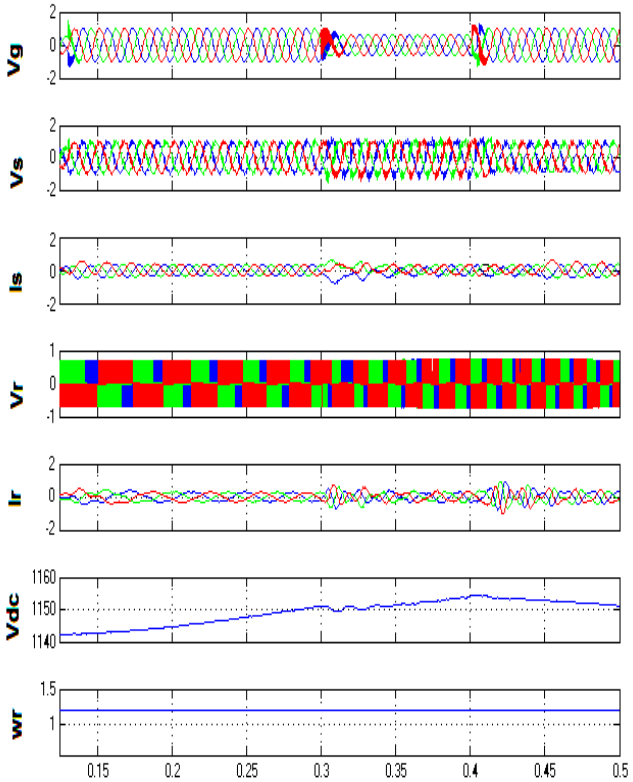

Fig. 13. Grid Voltage, stator voltage and current, Rotor voltage and current, dc link voltage, rotor speed for ANN controller based Nine switch inverter fed DFIG during LLLG fault

. It is observed that, using ANN controller the voltage injected at neutral side is pure sinusoidal waveform and DFIG injects 1.4 MW real power and 1.1 MVAR reactive power to grid.

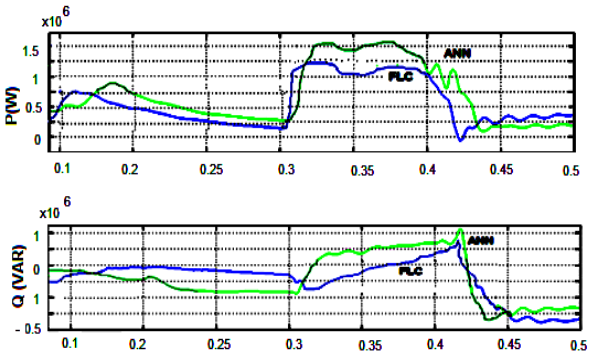

Fig. 14. Real power and reactive power injected to grid using ANN controller based Nine switch inverter fed DFIG during LLLG fault

The stator and rotor currents are limited to safe value within p.u below the transient current and there is no distortion during transient period as shown in Fig.13. At Fig.13, there are some small fluctuations in active and reactive power but the system recovers its good stability state. By inspection of the dynamic response, it can be realized that the dynamic response of the DFIG based wind system when provided with the ANN controllers has maximum percentage overshoot lower than that of experienced by the Fuzzy PI controllers. The ANN and fuzzy logic controllers improve the system damping after the first overshoot in compared with that of the PI controllers. It also yields a much faster response that allows the system to reach the steady state after 0.415s, while in the PI technique it reaches the steady state after 0.45s. Also the stator flux is limited within the value of p.u and NSC injects the p.u during fault period. In order to maintain the voltage stability, the value of real and reactive power injected by DFIG to grid is increased when compared with Fuzzy based controller during fault period of 0.3 to 0.4s.

Thus, an adequate control should have optimized operating point by control of active power supplied by the wind and controlled interchange of reactive power between the generator and the grid where in general the fluctuation in voltage occurs. This distortions can be reduced by using ANN based stator flux Controller, ANN based dc link voltage and ANN based Reactive power controller by reducing the Mean Squared Error. The real power and reactive power are injected during voltage dip for maintain the voltage profile. This paper proposed ANN based Fault tolerant control of nine switch converter based DFIG under LLLG fault and the improvement of voltage and current waveforms of stator and rotor quantities, real power and reactive power in injection , controlled stator flux within 1 p.u are shown in fig.11 to fig.13. The vector control with ANN based control is applied to DFIG in order to achieve the independent control of active and reactive power by decoupling the rotor current into quadrature ‘q’ and direct ‘d’ axis components[22]. The ANN controller with gains tuned with minimum steady state error, low overshoot and low ripples. The final results of the proposed controllers for DFIG show the superiority of the ANN versus the PI controller and Fuzzy based controller, which improves the time specification of the response in term of reducing steady state error, Integral Square Error(ISE) ,Integral of Absolute error(IAE) and smoother response and requires less time to reach steady state which makes this controller more robust to the variation in load and wide range of power other than the rest controllers.

Processing becomes simpler as computational complexity is reduced. The performance indices Integral of square of error(ISE) and Integral of Absolute Error(IAE),settling time of conventional PI , FLC based controllers and ANN controllers are shown in Table III and percentage of error reduction and settling time reduction in ANN based DFIG is shown in Table IV .

TABLE III PERFORMANCE INDICES OF CONTROLLERS

Types of controller	Conventional PI controller		FLC based controller		ANN based Controller	
	ISE	IAE	ISE	IAE	ISE	IAE
Stator Flux controller	0.1852	0.2699	0.167	0.2813	0.1573	0.2501
Reactive power controller	0.5881	0.4212	0.6154	0.4312	0.4711	0.3653
Vdc controller	8.49e-6	0.0013	5.96e-6	0.0015	4.9e-6	0.0011
Settling time	0.45		0.42		0.41	

TABLE V Co

TABLE IV Percentage error reduction and Settling time reduction in ANN based DFIG

Types of controller	% Error reduced in ANN based controller	
	ISE	IAE
Stator Flux controller	5.8%	11.09%
Reactive power controller	23.44%	15.2%
Vdc controller	17.78%	26.67%
Settling time	2.38% settling time is reduced in ANN based system	

Table V illustrates that the comparison of performace characteristics of DFIG with PI, fuzzy PI and ANN controller in terms of injected real power, reactive power and voltage during LLLG fault. The ANN controller

designed for DFIG has been connected to a variable speed wind Turbine.

TABLE V Comparison of Real, Reactive power and Voltage injected into Grid between Fuzzy PI and ANN based DFIG

Parameters injected to GRID	Conventional PI controller based DFIG	Fuzzy PI based DFIG	ANN based DFIG
Real Power **(MW)**	0.75	1.0	**1.4**
Reactive power **(MVAR)**	0.5	1.0	**1.1**
THD of injected voltage(%)	5.42	3.98	**3.34**

The grid-side and rotor-side converters reference voltages are optimization PI parameters. The comparative study between the two controllers shows that ANN is very effective on the stabilization of the system shown in Table III. The real and reactive power injected to grid during the LLLG fault is increased and distortion is reduced in ANN based intelligent control of Nine switch Grid side converter than conventional controller based Grid side converter as shown in Table V.

VI. CONCLUSION

One-third rating of the ANN based Grid Side Nine Switch converter fault-tolerant DFIG arrangement is proposed for novel FRT operation during LLLG fault. Moreover, the adequate control approaches for controlling stator flux and maintain the dc link voltage an injecting reactive power by the conventional PI based Dual Output Converter and ANN Intelligent controller based Nine switch Converter fed DFIG during steady-state and transient conditions are developed. The proposed ANN based fault-control DFIG in riding through the grid faults is evaluated through using simulation studies and effectiveness of ANN controller is evaluated by the measured value of ISE and IAE. The compensation and profit associated with the proposed ANN based configuration over other FRT techniques can be summarized as FRT, NSC injection voltage ,real and reactive power, economical solution with the use of three supplementary switches, without output filter. In the meantime, the model is simplified and the computation complexity is reduced.

REFERENCES

[1] European Commission, " *European smart grids technology platform*", 2006.

[2] A. Ipakchi, F. Albuyeh, "*Grid of the future*", IEEE Power Energy Magazin, 2009,pp. 52–62,.

[3] R Datta, V. T Ranganathan, " *Variable-Speed Wind Power Generation using Doubly Fed Wound Rotor InductionMachine – a Comparison with Alternative Schemes*", IEEE Transactions on Energy Conversion , Sep 2002,vol.No. 3(17) ,pp. 414–421.

[4] R. Pena, J.C. Clear, G.M. Asher, " *Doubly fed induction generator using back-to- back PWM converters and its application to variable-speed wind energy generation*", IEEE Proc.: Electr. Power Appl. 1996,143 (3) , 231–241,

[5] V. Akhmatov, "*Analysis of Dynamic Behavior of Electric Power Systems with Large Amount of Wind Power*", Ph.D. Dissertation, April. 2003,Technical University of Denmark, Kgs. Lyngby, Denmark,

[6] International Renewable EnergyAgency(IRENA), "*Scaling up variable renewable power: the role of grid codes*",2016.

[7] M Rahimi, M Parniani, " *Grid-fault ride-through analysis and control of wind turbines with doubly fed induction generators*",Electric Power Systems Research,2010, 80 (2), 184-195.

[8] Q. Wei, G. K. Venayagamoorthy, and R. G. Harley, "*Real-Time Implementation of a STATCOM on a Wind Farm Equipped With Doubly Fed Induction Generators*", Industry Applications,2009, IEEE Transactions *on*, vol. 45, pp. 98-107.

[9] A. F. Abdou, A. Abu-Siada, and H. R. Pota, "*Application of STATCOM to improve the LVRT of DFIG during RSC fire-through fault*", in *Universities*Power Engineering Conference (AUPEC), 2012,22nd Australasian, 2012, pp. 1-6.

[10] C. Liu, Y. Kang, J. Chen, L. Kevin, X. Lin, X. Liu, and F. Xu, "*Simplified Active and Reactive Power Control of Doubly Fed Induction Generator and the Simulation with STATCOM",in Applied Power Electronics Conference and Exposition*, 2009,Twenty-*Fourth Annual IEEE*, pp. 1927-1931.

[11] M. Ferdosian, H. Abdi, and A. Bazaei, "*Improved dynamic performance of wind energy conversion system by UPFC*", in Industrial Technology (ICIT), 2013, IEEE International Conference on, ,pp. 545- 550.

[12] M. T. Hagh, A. Lafzi, and A. R. Milani, "*Dynamic and stability improvement of a wind farm connected to grid using UPFC*," in Industrial Technology, 2008, IEEE International Conference, 2008, pp. 1-5.

[13] W. Zhang, P. Zhou, andY.He, "*Analysis of the by-pass resistance of an active crowbar for doubly-fed induction generator based wind turbines under grid faults*," in *Proc. Int. Conf. Electr. Mach. Syst. (ICEMS)*, Oct.2008, pp. 2316–2321.

[14] G. Pannell, D. Atkinson, and B. Zahawi, "*Minimum-threshold crowbar for a fault-ride-through grid-code-compliant DFIG wind turbine*," *IEEE Trans. Energy Convers.*, Sep. 2010,vol. 25, no. 3, pp. 750–759.

[15] J. Morren and S. de Haan, "*Short-circuit current of wind turbines with doubly fed induction generator*," *IEEE Trans. Energy Convers.*, , Mar. 2007vol.22, no. 1, pp. 174–180.

[16] J. Yang, J. Fletcher, and J. O'Reilly, "*A series-dynamic-resistor-basedconverter protection scheme for doubly-fed induction generator during various fault conditions*," *IEEE Trans. Energy Convers* ,Jun. 2010., vol. 25, no. 2,pp. 422–432.

[17] M. Mohseni, S. Islam, and M. A. S. Masoum, "*Fault ride-through capability enhancement of doubly-fed induction wind generators*," *IETRenew. Power Generat.*, Jul. 2011,vol. 5, no. 5, pp. 368–376.

[18] P. Kanjiya, B. Ambati, and V. Khadkikar, "*A novel fault-tolerant dfigbased wind energy conversion system for seamless operation during grid faults*,"IEEETrans.PowerSyst., May2014,vol.29,no.3,pp.1296–1305.

[19] L.Zhang,P.C.Loh,andF.Gao,"*An integrated nine-switch power conditioner for power quality enhancement and voltage sag mitigation*," IEEE Trans. Power Electron., Mar. 2012vol. 27, no. 3, pp. 1177–1190.

[20] Hornik, M. Stinchcombe and H. White, "*Multilayer feed forward networks are universal approximators*", Neural Networks,1989, vol. 2, pp. 359-366,.

[21] Vadirajacharya G. Kinhal, Promod Agarwal and Hari Oam Gupta, "*performance Investigation of Neural Network Based Unified Power-Quality Conditioner*", IEEE Transactions on power delivery, Jan. 2011, vol. 26, no. 1, ,pp.431-437.

[22] R. Kumar, R. A. Gupta, S.V. Bhangale, and H. Gothwal, "*Artificial neural network based direct torque control of induction motor*

drives", IETECH Journal of Electrical Analysis, 2008,vol. 2, no. 3, IETECH Publications, pp.159-165.

M. Nirmala received her B.E degree in Electrical and Electronics Engineering from Bharathiyar University, India in 2001 and M.E degree in Power Electronics and Drives from Anna University Chennai, India in 2006. She is currently working as Senior Grade Assistant Professor(SRG) in Kumaraguru College Of Technology, Coimbatore, India. . Her Main research is in Power Quality improvements in Wind energy conversion system and her area of interest is applications Power Electronics, Renewable Energy sources, Smart Grid, Load side Management in Distribution.

Dr.K.Baskaran received his Bachelor of Engineering in Electrical and Electronics Engineering from the Annamalai University, India in 1989, Master of Engineering in Computer Science Engineering from Bharathiar University, India in 2002.and Ph. D degree from Anna University-Chennai, India in of IEEE and member of ISTE. He is Associate Professor in Electrical and Electronics Engineering, Government college of Technology, Coimbatore, India. His area of interest includes Adhoc networks, network security, electrical system control, power quality, smart grid,etc.,